International Journal of Control, Automation, and Systems (2015) 13(4):926-933 ISSN:1598-6446 eISSN:2005-4092
DOI 10.1007/s12555-014-0564-8 http://www.springer.com/12555

Dynamic Modeling of a Two-wheeled Inverted Pendulum Balancing Mobile Robot

Sangtae Kim and SangJoo Kwon*

Abstract: Many of the currently available dynamic models for the two-wheeled balancing mobile robot have some common mistakes, which are mainly due to misunderstanding about the coordinate systems to describe the rotating motions and a lack of rigorous comparison with former derivations. This paper investigates the modeling procedures for the 2WBMR in terms of the Lagrangian approach and Kane's method, through which an exact dynamic model is given, and we discuss how the modeling errors in the former works were induced. Numerical examples are given to see the effect of the erroneous terms on the postural stability.

Keywords: Balancing robot, inverted pendulum robot, Kane's method, nonholonomic constraint.

1. INTRODUCTION

Two-wheeled balancing mobile robot (2WBMR) or inverted pendulum robot belongs to a nonlinear system which consists of a two-wheeled chassis and inverted pendulum body. It is an interesting underactuation system which implements the three degrees-of-freedom motion including pitch, yaw and straight movement with only two wheels' rotations. The 2WBMR has drawn much attention for the past fifteen years because of its compact design and versatility in congested urban areas.

Although the 2WBMRs are unfavorable in postural stability because of the inherent inverted pendulum structure, it has many advantages in the respect of driving efficiency. For example, it can pass through narrow spaces unlike three wheelers or four wheelers and enables the driver to steer on a spot and maintain an upright posture on inclined terrains. Hence, the 2WBMR platforms are being widely applied, from unmanned navigation vehicles [1-4] to personal transporters [5-9] and even to robot wheelchairs for the disabled [10,11].

For the design purpose of a 2WBMR, it is necessary to evaluate the driving performance and stability through parametric study. Specifically, the self-tilt-up balancing robot using a reaction wheel [12] and the wheeled humanoid [13] show the critical role of dynamic model in the design process. A reliable dynamic model is a prerequisite requirement for the model-based control designs such as adaptive control [5,14], fuzzy logic control [15], and sliding model control [16]. The characteristics of the 2WBMR can be better understood by dynamic analysis [3], model identification [8], and controllability analysis [17]. Also, relevant algorithm designs of trajectory generation [18] and obstacle avoidance [19] can be assisted by appropriate dynamic models.

There are three possible ways to get the dynamic model of a 2WBMR. First, the Newtonian approach goes through rather a complicated process of considering interactive forces between the constituent bodies, but it provides an intuitive understanding about the robot motion by dealing with vector relationships between forces and accelerations [2,12,15,20]. Secondly, the Lagrangian approach is the most popular for the modeling of a multibody system, where the equation of motion can be readily derived as far as the kinetic energy and potential energy are defined as the functions of generalized coordinates [1,6,8,13,14,16,17,21,22]. Thirdly, Kane's method [23] is also based on vector operations like Newtonian mechanics, but it doesn't have to find interactive forces between the rigid bodies. Instead, it determines generalized inertia forces and generalized active forces by means of the partial velocities along the generalized coordinates [3,7,24].

Actually, great progress has been made on the two-wheeled balancing robot technology. But, many of the existing articles are suggesting dynamic models with wrong or missing terms and those mistakes are being repeated in the follow-on works. Taking an example, a 3-DOF model of the inverted pendulum robot was derived in [2] by applying Newtonian mechanics. However, it omitted some components in the centrifugal and Coriolis forces by neglecting the lateral motion of the pendulum body. Therefore, the results in [5] which utilized its dynamic model in their adaptive control design are questionable in reliability. The same dynamic model was consulted in [20], but it escaped from the modeling errors since only 2-D motions were considered excepting yaw motion.

Manuscript received December 24, 2014; revised January 10, 2015; accepted January 12, 2015. Recommended by Associate Editor Kyu-Jin Cho under the direction of Editor Hyouk Ryeol Choi.

This research was supported by Basic Science Research Program through the National Research Foundation of Korea (NRF-2012R1A1B3003886).

Sangtae Kim and SangJoo Kwon are with the School of Aerospace and Mechanical Engineering, Korea Aerospace University, Goyang 412-791, Korea (e-mails: {kimmonkey, sjkwon}@kau.ac.kr).

* Corresponding author.

The modeling errors in the previous studies were caused because they lacked sound understanding about the rotational motion of the inverted pendulum body and a concrete comparison with former derivations. This paper investigates the dynamic model of a 2WBMR in terms of Lagrangian approach and Kane's method, where the modeling procedures are rigorously compared and it is discussed what made the modeling errors in other works. As well, the effects of the missing terms concerned with the mass moment of inertia and Coriolis acceleration are analyzed through numerical examples.

2. KINEMATICS OF 2WBMR

2.1. Kinematic constraints

From a modeling point of view, the 2WBMR consists of three rigid bodies with two wheels on the left and right and an inverted pendulum as shown in Fig. 1, where $\{N\}$ denotes the Newtonian frame fixed in space, $\{C\}$ the chassis frame attached at the center of the wheel axis, and $\{B\}$ the body frame whose origin is located at the center of mass of the inverted pendulum. The whole body of the robot moves together by straight motion and yaw rotation and the inverted pendulum has additional pitch motion. The transformation matrices between the frames can be written as

$$ {}^{N}R_{C}(\psi)=\begin{bmatrix} \mathrm{c}\psi & -\mathrm{s}\psi & 0 \\ \mathrm{s}\psi & \mathrm{c}\psi & 0 \\ 0 & 0 & 1 \end{bmatrix},\quad {}^{C}R_{B}(\theta)=\begin{bmatrix} \mathrm{c}\theta & 0 & \mathrm{s}\theta \\ 0 & 1 & 0 \\ -\mathrm{s}\theta & 0 & \mathrm{c}\theta \end{bmatrix}, \tag{1} $$

where ${}^{i}R_{j}$ represents the rotation from i-frame to j-frame, $\mathrm{s}\theta=\sin\theta$, and $\mathrm{c}\theta=\cos\theta$.

The main model parameters of 2WBMR are listed in Table 1 and the other notations in Fig. 1 indicate that (L, R, B):
Left wheel, right wheel, inverted pendulum body
$\hat{\omega}^{L},\hat{\omega}^{R},\hat{\omega}^{B}$: Angular velocities of (L, R, B)
$\hat{v}^{L},\hat{v}^{R},\hat{v}^{B}$: Velocities of the centers of mass of (L, R, B)
$\hat{v}^{C},\hat{\omega}^{C}$: Linear and angular velocity of the $\{C\}$ frame
T_L,T_R : Wheel torques exerted at (L, R)
f_L,f_R : Damping torques generated at (L, R)
$\dot{x},\dot{\theta},\dot{\psi}$: Forward velocity, pitch rate, yaw rate
γ_L,γ_R : Rotation angles of (L, R)

In order to fully describe the motion of the three rigid bodies, totally thirteen generalized coordinates: x_B, y_B, z_B, x_L, y_L, x_R, y_R, x_C, y_C, γ_L, γ_R, θ, ψ are necessary as denoted in Fig. 2. However, with respect to the fixed reference frame $\{N\}$, the center of mass of each body is governed by the holonomic constraints:

$$ \begin{aligned} &x_B = x_C + l\,\mathrm{s}\theta\,\mathrm{c}\psi, \quad y_B = y_C + l\,\mathrm{s}\theta\,\mathrm{s}\psi, \quad z_B = l\,\mathrm{c}\theta, \\ &x_L = x_C - (d/2)\mathrm{s}\psi, \quad y_L = y_C + (d/2)\mathrm{c}\psi, \\ &x_R = x_C + (d/2)\mathrm{s}\psi, \quad y_R = y_C - (d/2)\mathrm{c}\psi. \end{aligned} \tag{2} $$

Assuming that there is no slip on the ground, the differential motions of the generalized coordinates have the geometric relationships in Fig. 3. That is, the translational velocity of each wheel is determined by the radius of the wheel and its rotational velocity, and the yaw angle of the chassis is constrained by the ratio of the velocity components. Hence, we have the nonholonomic constraints in non-integrable forms:

$$ \begin{aligned} &\dot{x}_L\,\mathrm{c}\psi + \dot{y}_L\,\mathrm{s}\psi = r\dot{\gamma}_L, \\ &\dot{x}_R\,\mathrm{c}\psi + \dot{y}_R\,\mathrm{s}\psi = r\dot{\gamma}_R, \\ &(\dot{x}_L + \dot{x}_R)\mathrm{s}\psi = (\dot{y}_L + \dot{y}_R)\mathrm{c}\psi, \end{aligned} \tag{3} $$

which are equivalent to

$$ \begin{aligned} &\dot{x}_C\,\mathrm{c}\psi + \dot{y}_C\,\mathrm{s}\psi - (d/2)\dot{\psi} - r\dot{\gamma}_L = 0, \\ &\dot{x}_C\,\mathrm{c}\psi + \dot{y}_C\,\mathrm{s}\psi + (d/2)\dot{\psi} - r\dot{\gamma}_R = 0, \\ &\dot{x}_C\,\mathrm{s}\psi - \dot{y}_C\,\mathrm{c}\psi = 0. \end{aligned} \tag{4} $$

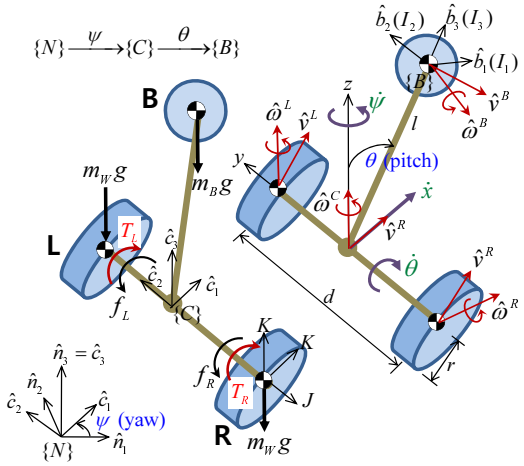

Fig. 1. Schematic of the two-wheeled inverted pendulum robot.

Table 1. Model parameters of 2WBMR.

Symbol	Definition
d	Distance between the two wheels
l	Length of pendulum
r	Radius of wheels
m_B	Mass of the pendulum body (except wheels)
m_W	Mass of each wheel
J, K	Mass moment of inertia (MOI) of each wheel w.r.t. the wheel axis and the vertical axis
I_1, I_2, I_3	MOI of the pendulum body w.r.t. $\{B\}$

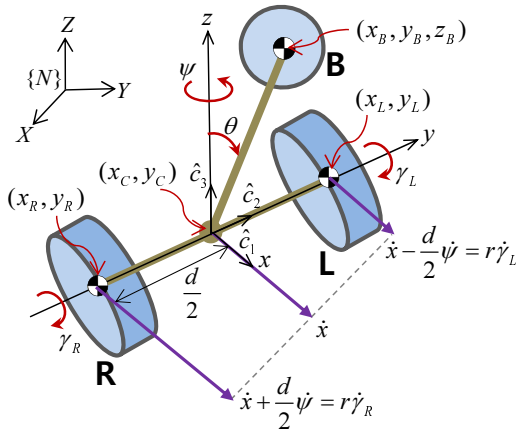

Fig. 2. Thirteen generalized coordinates of 2WBMR.

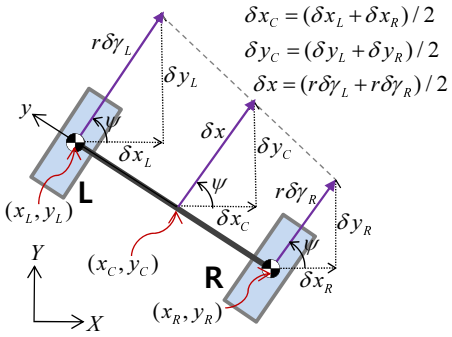

Fig. 3. Differential motion constraints in the two-wheeled motion.

If we apply the relationships of the seven holonomic constraints in (2) and the three nonholonomic ones in (4) to the thirteen generalized coordinates in Fig. 2, it is confirmed that the 2WBMR has the mobility of three degrees of freedom.

2.2. Linear and angular velocities of rigid bodies

Summing the first two equations in (4), the forward velocity of the chassis has the constraint of

$$\dot{x} = \dot{x}_C \,\mathrm{c}\psi + \dot{y}_C \,\mathrm{s}\psi. \tag{5}$$

Then, from (4), we have

$$\dot{\gamma}_L = \frac{\dot{x} - (d/2)\dot{\psi}}{r}, \quad \dot{\gamma}_R = \frac{\dot{x} + (d/2)\dot{\psi}}{r}, \tag{6}$$

which indicates that under no slip condition, the rotational velocities of the left and right wheels are constrained by the forward velocity of the robot and the yaw rate.

By differentiating both sides of (2), the velocity components of $\{L, R, B\}$ can be determined with respect to $\{N\}$. As a consequence, we have

$$\begin{aligned}
\hat{v}^L &= \left(\dot{x}_C - (d/2)\dot{\psi}\,\mathrm{c}\psi\right)\hat{n}_1 + \left(\dot{y}_C - (d/2)\dot{\psi}\,\mathrm{s}\psi\right)\hat{n}_2, \\
\hat{v}^R &= \left(\dot{x}_C + (d/2)\dot{\psi}\,\mathrm{c}\psi\right)\hat{n}_1 + \left(\dot{y}_C + (d/2)\dot{\psi}\,\mathrm{s}\psi\right)\hat{n}_2, \\
\hat{v}^B &= (\dot{x}_C + l\dot{\theta}\,\mathrm{c}\theta\,\mathrm{c}\psi - l\dot{\psi}\,\mathrm{s}\theta\,\mathrm{s}\psi)\hat{n}_1 \\
&\quad + (\dot{y}_C + l\dot{\theta}\,\mathrm{c}\theta\,\mathrm{s}\psi + l\dot{\psi}\,\mathrm{s}\theta\,\mathrm{c}\psi)\hat{n}_2 - (l\dot{\theta}\,\mathrm{s}\theta)\hat{n}_3.
\end{aligned} \tag{7}$$

Considering transformations among the frames in Fig. 1, the angular velocities of the three bodies can be expressed with respect to the moving frames as

$$\begin{aligned}
\hat{\omega}^L &= \hat{\omega}^C + \dot{\gamma}_L\hat{c}_2 = \dot{\psi}\hat{c}_3 + (1/r)\left(\dot{x} - d\dot{\psi}/2\right)\hat{c}_2, \\
\hat{\omega}^R &= \hat{\omega}^C + \dot{\gamma}_R\hat{c}_2 = \dot{\psi}\hat{c}_3 + (1/r)\left(\dot{x} + d\dot{\psi}/2\right)\hat{c}_2, \\
\hat{\omega}^B &= \hat{\omega}^C + \dot{\theta}\hat{b}_2 = (-\dot{\psi}\,\mathrm{s}\theta)\hat{b}_1 + \dot{\theta}\hat{b}_2 + (\dot{\psi}\,\mathrm{c}\theta)\hat{b}_3.
\end{aligned} \tag{8}$$

In the same way, the linear velocities can be expressed in the moving frames as

$$\begin{aligned}
\hat{v}^L &= \hat{v}^C + {}^C\hat{v}^L = \dot{x}\hat{c}_1 + \hat{\omega}^C \times \left(d/2\right)\hat{c}_2 = \left(\dot{x} - d\dot{\psi}/2\right)\hat{c}_1, \\
\hat{v}^R &= \hat{v}^C + {}^C\hat{v}^R = \dot{x}\hat{c}_1 + \hat{\omega}^C \times \left(-d/2\right)\hat{c}_2 = \left(\dot{x} + d\dot{\psi}/2\right)\hat{c}_1, \\
\hat{v}^B &= \hat{v}^C + {}^C\hat{v}^B = \dot{x}\hat{c}_1 + \hat{\omega}^B \times l\hat{b}_3 = \dot{x}\hat{c}_1 + (l\dot{\theta})\hat{b}_1 + (l\dot{\psi}\,\mathrm{s}\theta)\hat{b}_2,
\end{aligned} \tag{9}$$

where $({}^C\hat{v}^L, {}^C\hat{v}^R, {}^C\hat{v}^B)$ means the relative velocities of (L, R, B) with respect to the $\{C\}$ frame.

3. LAGRANGIAN APPROACH

3.1. Lagrangian equation of motion with constraints

In applying the Lagrangian modeling approach, we need to express the kinetic energy and potential energy of the three rigid bodies as the functions of generalized coordinates. First, the translational kinetic energy of the 2WBMR in Fig. 1 can be written as

$$T_{trans} = \frac{1}{2}m_W(\hat{v}^L \cdot \hat{v}^L) + \frac{1}{2}m_W(\hat{v}^R \cdot \hat{v}^R) + \frac{1}{2}m_B(\hat{v}^B \cdot \hat{v}^B). \tag{10}$$

By using the mass moment of inertia (MOI) of the two wheels and the inverted pendulum denoted in Fig. 1, the rotational kinetic energy is given by

$$T_{rot} = \frac{1}{2}(\hat{\omega}^L)^T\hat{I}_L\hat{\omega}^L + \frac{1}{2}(\hat{\omega}^R)^T\hat{I}_R\hat{\omega}^R + \frac{1}{2}(\hat{\omega}^B)^T\hat{I}_B\hat{\omega}^B, \tag{11}$$

where if the robot body is symmetrical, the inertia matrices have the diagonal forms:

$$\hat{I}_L = \hat{I}_R = \mathrm{diag}\{K, J, K\}, \quad \hat{I}_B = \mathrm{diag}\{I_1, I_2, I_3\}. \tag{12}$$

By substituting (8) into (11), we have

$$\begin{aligned}
T_{rot} &= \frac{1}{2}\left((I_1 - I_3)\mathrm{s}^2\theta + I_3 + 2K\right)\dot{\psi}^2 + \frac{1}{2}I_2\dot{\theta}^2 \\
&\quad + \frac{1}{2}J(\dot{\gamma}_L^2 + \dot{\gamma}_R^2).
\end{aligned} \tag{13}$$

When the 2WBMR is moving on a plane, the vertical motion happens only by the pitch motion of inverted pendulum. Thus, the potential energy of 2WBMR is

$$V = m_B g l\,\mathrm{c}\theta. \tag{14}$$

Now, the Lagrangian is defined by

$$L = T - V = T_{trans} + T_{rot} - V. \tag{15}$$

If we substitute the linear velocities in (7) into (10), the above Lagrangian becomes the function of the following six generalized coordinates

$$q_1 = x_C,\ q_2 = y_C,\ q_3 = \theta,\ q_4 = \psi,\ q_5 = \gamma_L,\ q_6 = \gamma_R. \tag{16}$$

Now, the Lagrangian equation of motion is given by

$$\frac{d}{dt}\left(\frac{\partial L}{\partial \dot{q}_i}\right) - \frac{\partial L}{\partial q_i} = Q_i + \sum_j \lambda_j a_{ji} \left(i = 1 \sim 6, j = 1 \sim 3\right), \tag{17}$$

where the nonholonomic constraints in (4) are involved through the Lagrangian multipliers with

$$\begin{aligned}
a_{1i} &= \frac{\partial}{\partial \dot{q}_i}\left(\dot{x}_C\,\mathrm{c}\psi + \dot{y}_C\,\mathrm{s}\psi - \frac{d}{2}\dot{\psi} - r\dot{\gamma}_L\right), \\
a_{2i} &= \frac{\partial}{\partial \dot{q}_i}\left(\dot{x}_C\,\mathrm{c}\psi + \dot{y}_C\,\mathrm{s}\psi + \frac{d}{2}\dot{\psi} - r\dot{\gamma}_R\right),
\end{aligned} \tag{18}$$

$$a_{3i} = \frac{\partial}{\partial \dot{q}_i}\left(\dot{x}_C \,\mathrm{s}\psi - \dot{y}_C \,\mathrm{c}\psi\right)$$

for $i = 1 \sim 6$. On the other hand, the generalized forces corresponding to the generalized coordinates can be written as

$$\begin{aligned} &Q_1 = Q_2 = Q_4 = 0, \quad Q_3 = -(Q_5 + Q_6), \\ &Q_5 = T_L - f_L = T_L - c_\alpha(\dot{\gamma}_L - \dot{\theta}), \\ &Q_6 = T_R - f_R = T_R - c_\alpha(\dot{\gamma}_R - \dot{\theta}), \end{aligned} \tag{19}$$

where c_α is the coefficient of viscous friction on the wheel axis. It should be noted that the damping torque is proportional to the relative angular velocity between the RPM of a wheel, and the pitch rate and the generalized force Q_3 for the pitch motion is equivalent to the reaction to the wheel torques.

By expanding (17) for the generalized coordinates in (16), we have

$$\begin{aligned} &m_B\begin{pmatrix} \ddot{x}_C + l\ddot{\theta}\,\mathrm{c}\theta\,\mathrm{c}\psi - l\ddot{\psi}\,\mathrm{s}\theta\,\mathrm{s}\psi \\ -2l\dot{\theta}\dot{\psi}\,\mathrm{c}\theta\,\mathrm{s}\psi - l(\dot{\theta}^2 + \dot{\psi}^2)\,\mathrm{s}\theta\,\mathrm{c}\psi \end{pmatrix} + 2m_W\ddot{x}_C \\ &= \lambda_1\,\mathrm{c}\psi + \lambda_2\,\mathrm{c}\psi + 2\lambda_3\,\mathrm{s}\psi, \quad i = 1(x_C), \end{aligned} \tag{20}$$

$$\begin{aligned} &m_B\begin{pmatrix} \ddot{y}_C + l\ddot{\theta}\,\mathrm{c}\theta\,\mathrm{s}\psi + l\ddot{\psi}\,\mathrm{s}\theta\,\mathrm{c}\psi \\ +2l\dot{\theta}\dot{\psi}\,\mathrm{c}\theta\,\mathrm{c}\psi - l(\dot{\theta}^2 + \dot{\psi}^2)\,\mathrm{s}\theta\,\mathrm{s}\psi \end{pmatrix} + 2m_W\ddot{y}_C \\ &= \lambda_1\,\mathrm{s}\psi + \lambda_2\,\mathrm{s}\psi - 2\lambda_3\,\mathrm{c}\psi, \quad i = 2(y_C), \end{aligned} \tag{21}$$

$$\begin{aligned} &m_B\left(\ddot{x}_C\,\mathrm{c}\psi + \ddot{y}_C\,\mathrm{s}\psi\right)l\,\mathrm{c}\theta + (I_2 + m_B l^2)\ddot{\theta} \\ &\quad - (I_1 - I_3 + m_B l^2)\dot{\psi}^2\,\mathrm{s}\theta\,\mathrm{c}\theta - m_B g l\,\mathrm{s}\theta \\ &= -(T_L + T_R) + c_\alpha(\dot{\gamma}_L - \dot{\theta}) + c_\alpha(\dot{\gamma}_R - \dot{\theta}), \; i = 3(\theta), \end{aligned} \tag{22}$$

$$\begin{aligned} &\left\{I_3 + m_W d^2/2 + 2K + (I_1 - I_3)\,\mathrm{s}^2\theta\right\}\ddot{\psi} \\ &\quad + m_B\left\{-\ddot{x}_C\,\mathrm{s}\psi + \ddot{y}_C\,\mathrm{c}\psi - (\dot{x}_C\,\mathrm{c}\psi + \dot{y}_C\,\mathrm{s}\psi)\dot{\psi}\right\}l\,\mathrm{s}\theta \\ &\quad + m_B(\dot{x}_C\,\mathrm{c}\psi + \dot{y}_C\,\mathrm{s}\psi)\dot{\psi}l\,\mathrm{s}\theta + 2(I_1 - I_3)\dot{\theta}\dot{\psi}\,\mathrm{s}\theta\,\mathrm{c}\theta \\ &= -d\lambda_1/2 + d\lambda_2/2, \quad i = 4(\psi), \end{aligned} \tag{23}$$

$$J\ddot{\gamma}_L = -r\lambda_1 + T_L - c_\alpha(\dot{\gamma}_L - \dot{\theta}), \quad i = 5(\gamma_L), \tag{24}$$

$$J\ddot{\gamma}_R = -r\lambda_2 + T_R - c_\alpha(\dot{\gamma}_R - \dot{\theta}), \quad i = 6(\gamma_R).$$

3.2. 3-DOF dynamic model for 2WBMR

Now, the Lagrangian multipliers can be eliminated by finding λ_1 and λ_2 in (24) and substituting them into (20)-(23) and then solving λ_3 from (20) and (21). Finally, if we apply the relationships in (5) and (6), we have three independent nonlinear equations of motion for a 2WBMR with respect to the generalized coordinates (x, θ, ψ) as follows:

$$\begin{aligned} &\{m_B + 2m_W + 2J/r^2\}\ddot{x} - m_B l(\dot{\psi}^2 + \dot{\theta}^2)\,\mathrm{s}\theta \\ &\quad + (m_B l\,\mathrm{c}\theta)\ddot{\theta} + (2/r)c_\alpha(\dot{x}/r - \dot{\theta}) = (T_L + T_R)/r, \end{aligned} \tag{25}$$

$$\begin{aligned} &(I_2 + m_B l^2)\ddot{\theta} + (m_B l\,\mathrm{c}\theta)\ddot{x} + (I_3 - I_1 - m_B l^2)\dot{\psi}^2\,\mathrm{s}\theta\,\mathrm{c}\theta \\ &\quad - m_B l g\,\mathrm{s}\theta - 2c_\alpha(\dot{x}/r - \dot{\theta}) = -(T_L + T_R), \end{aligned} \tag{26}$$

$$\begin{aligned} &\left\{I_3 + 2K + m_W\frac{d^2}{2} + J\frac{d^2}{2r^2} - (I_3 - I_1 - m_B l^2)\,\mathrm{s}^2\theta\right\}\ddot{\psi} \\ &\quad + \left\{m_B l\dot{x} - 2(I_3 - I_1 - m_B l^2)\dot{\theta}\,\mathrm{c}\theta\right\}\dot{\psi}\,\mathrm{s}\theta \\ &\quad + c_\alpha\dot{\psi}d^2/(2r^2) = (T_R - T_L)d/(2r). \end{aligned} \tag{27}$$

By arranging the above equations in matrix form, we have

$$M(q)\ddot{q} + C(q,\dot{q})\dot{q} + D\dot{q} + G(q) = B\tau, \tag{28}$$

where inertia matrix M, centrifugal and Coriolis matrix C, damping matrix D, gravity vector G, input matrix B, input vector τ, and generalized coordinates q have the following forms, respectively, with the elements given in Appendix A.

$$\begin{aligned} &M = \begin{bmatrix} a_{11} & a_{12} & 0 \\ a_{21} & a_{22} & 0 \\ 0 & 0 & a_{33} \end{bmatrix}, \; C = \begin{bmatrix} 0 & c_{12} & c_{13} \\ 0 & 0 & c_{23} \\ c_{31} & c_{32} & c_{33} \end{bmatrix}, \; q = \begin{bmatrix} x \\ \theta \\ \psi \end{bmatrix}, \\ &D = \begin{bmatrix} d_{11} & d_{12} & 0 \\ d_{21} & d_{22} & 0 \\ 0 & 0 & d_{33} \end{bmatrix}, \; B = \begin{bmatrix} 1/r & 1/r \\ -1 & -1 \\ -d/2r & d/2r \end{bmatrix}, \\ &\tau = \begin{bmatrix} T_L \\ T_R \end{bmatrix}, \; G = \begin{bmatrix} 0 & -m_B l g\,\mathrm{s}\theta & 0 \end{bmatrix}^T. \end{aligned} \tag{29}$$

3.3. Christoffel symbols

In (28), actually there exist an infinite number of choices in determining the centrifugal and Coriolis matrix for the given generalized coordinates. In general Euler-Lagrange systems, the inertia matrix is symmetric and $\dot{M} - 2C$ is skew symmetric. That is,

$$M = M^T, \quad \dot{M} - 2C = -(\dot{M} - 2C)^T. \tag{30}$$

However, the above properties are satisfied only if the elements of the centrifugal and Coriolis matrix follow the definition of Christoffel symbols for the inertia matrix [25]:

$$c_{ij} = \sum_{k=1}^{n}\frac{1}{2}\left(\frac{\partial m_{ij}}{\partial q_k} + \frac{\partial m_{ik}}{\partial q_j} - \frac{\partial m_{jk}}{\partial q_i}\right)\dot{q}_k \quad (i, j = 1 \sim n) \tag{31}$$

with n the number of generalized coordinates.

However, the above equation cannot be applied to the inertia matrix in (28) because some mass elements in (23) concerned with the yaw motion are removed in reflecting the nonholonomic constraints. In nonholonomic systems such as the wheeled mobile robot, the Christoffel symbol is valid only when the nonholonomic constraints are explicitly involved in the equations of motion like (20)-(24).

3.4. Lagrangian modeling errors in other works

When a 2WBMR is moving, the viscous friction on the wheel axis is exerted as a damping torque. According to the principle of action and reaction between the two rigid bodies, the damping torque to the wheels and the

inverted pendulum body must be the same, which is indicated in (19), and it resulted in (25) and (26). In [1], however, the damping torques were regarded as different when they considered the dissipative energy of the robot. Eventually, it led to an error in the dynamic model and arrived at the wrong conclusion that a certain pitch angle is necessary to keep uniform velocity of the robot. Furthermore, that misinformation was delivered to numerous follow-on works including [3,4,7,8,12-16,21,22,24].

The yaw motion of 2WBMR is generated by the velocity difference between the two wheels, and the angular velocity of the inverted pendulum is naturally the sum of the pitch rate and the yaw rate. However, in [8,22], the yaw rate direction was wrongly used with respect to $\{B\}$ as $\hat{\omega}^B = \dot{\theta}\hat{b}_2 + \dot{\psi}\hat{b}_3$ in determining the rotational kinetic energy, although it must be described with respect to $\{C\}$ as $\hat{\omega}^B = \dot{\theta}\hat{b}_2 + \dot{\psi}\hat{c}_3 = (-\dot{\psi}\,\mathrm{s}\,\theta)\hat{b}_1 + \dot{\theta}\hat{b}_2 + (\dot{\psi}\,\mathrm{c}\,\theta)\hat{b}_3$. After all, most of terms in the centrifugal and Coriolis force disappeared from their resulting equations of motion.

4. KANE'S METHOD

4.1. Partial velocities and partial angular velocities

Kane's method [23] provides rather a straightforward way to derive the equation of motion for a multi-body system by means of systematic vector operations. Instead of determining energy functions in Lagrangian approaches or examining interactive forces in Newtonian mechanics, it is based on finding generalized active forces and generalized inertia forces as the functions of generalized coordinates.

Following the procedure suggested in [23], first we define the generalized velocities for the straight, pitch, and yaw motion of a 2WBMR as

$$u_1 = \dot{x}, \quad u_2 = \dot{\theta}, \quad u_3 = \dot{\psi}. \tag{32}$$

The velocity and angular velocity of each rigid body can be expressed as

$$\hat{v}^P = \sum_{r=1}^{3} \hat{v}_r^P u_r, \quad \hat{\omega}^P = \sum_{r=1}^{3} \hat{\omega}_r^P u_r \quad (P = L, R, B), \tag{33}$$

where the partial velocities and partial angular velocities can be determined as

$$\hat{v}_r^P = \frac{\partial \hat{v}^P}{\partial u_r}, \ \hat{\omega}_r^P = \frac{\partial \hat{\omega}^P}{\partial u_r} \ (r = 1 \sim 3, \ P = L, R, B) \tag{34}$$

by taking the partial differentiations for the velocity and angular velocity with respect to the generalized velocities.

Then, by applying (34) to (8) and (9), we have

$$\begin{aligned}
&\hat{v}_1^L = \hat{c}_1 && \hat{v}_2^L = 0 && \hat{v}_3^L = (-d/2)\hat{c}_1 \\
&\hat{v}_1^R = \hat{c}_1 && \hat{v}_2^R = 0 && \hat{v}_3^R = (d/2)\hat{c}_1 \\
&\hat{v}_1^B = \hat{c}_1 && v_2^B = l\hat{b}_1 && \hat{v}_3^B = (l\,\mathrm{s}\,\theta)\hat{b}_2,
\end{aligned} \tag{35a}$$

$$\begin{aligned}
&\hat{\omega}_1^L = (1/r)\hat{c}_2 && \hat{\omega}_2^L = 0 && \hat{\omega}_3^L = -(d/2r)\hat{c}_2 + \hat{c}_3 \\
&\hat{\omega}_1^R = (1/r)\hat{c}_2 && \hat{\omega}_2^R = 0 && \hat{\omega}_3^R = (d/2r)\hat{c}_2 + \hat{c}_3 \\
&\hat{\omega}_1^B = 0 && \hat{\omega}_2^B = \hat{b}_2 && \hat{\omega}_3^B = \hat{c}_3.
\end{aligned} \tag{35b}$$

4.2. Generalized forces and torques

As indicated in Fig. 1, the active forces exerted at each rigid body are their weights, and the active torques are the actuator torque and the damping torque at each wheel. Hence,

$$\hat{R}_L = -m_W g\hat{n}_3, \quad \hat{R}_R = -m_W g\hat{n}_3, \quad \hat{R}_B = -m_B g\hat{n}_3, \tag{36a}$$

$$\begin{aligned}
\hat{\tau}_L &= (T_L - f_L)\hat{c}_2 = \left(T_L - c_\alpha(\dot{\gamma}_L - \dot{\theta})\right)\hat{c}_2, \\
\hat{\tau}_R &= (T_R - f_R)\hat{c}_2 = \left(T_R - c_\alpha(\dot{\gamma}_R - \dot{\theta})\right)\hat{c}_2, \\
\hat{\tau}_B &= -\left(T_L + T_R - 2c_\alpha(\dot{x}/r - \dot{\theta})\right)\hat{c}_2.
\end{aligned} \tag{36b}$$

The generalized active forces produce accelerations in the generalized coordinates. They can be determined by taking the inner product between the partial velocities and partial angular velocities (35) and the active forces and active torques (36) as follows:

$$F_r = \sum_{P=L,R,B} \hat{v}_r^P \cdot \hat{R}_P + \sum_{P=L,R,B} \hat{\omega}_r^P \cdot \hat{T}_P \ (r = 1 \sim 3), \tag{37}$$

which results in

$$\begin{aligned}
F_1 &= (1/r)\left(T_L + T_R - 2c_\alpha(\dot{x}/r - \dot{\theta})\right), \\
F_2 &= m_B l g\,\mathrm{s}\,\theta - \left(T_L + T_R - 2c_\alpha(\dot{x}/r - \dot{\theta})\right), \\
F_3 &= (d/2r)\left(T_R - T_L - c_\alpha(d/r)\dot{\psi}\right).
\end{aligned} \tag{38}$$

While, the mass moments of inertia of the three rigid bodies are given in dyadic forms:

$$\begin{aligned}
\hat{I}_L &= \hat{I}_R = K\hat{c}_1 \cdot \hat{c}_1 + J\hat{c}_2 \cdot \hat{c}_2 + K\hat{c}_3 \cdot \hat{c}_3, \\
\hat{I}_B &= I_1\hat{b}_1 \cdot \hat{b}_1 + I_2\hat{b}_2 \cdot \hat{b}_2 + I_3\hat{b}_3 \cdot \hat{b}_3,
\end{aligned} \tag{39}$$

and the accelerations and angular accelerations can be determined by differentiating (8) and (9) with respect to time.

Then, the inertia forces and inertia torques generating at each rigid body can be written as

$$\hat{R}_L^* = -m_W\hat{a}^L, \quad \hat{R}_R^* = -m_W\hat{a}^R, \quad \hat{R}_B^* = -m_B\hat{a}^B, \tag{40a}$$

$$\begin{aligned}
\hat{T}_L^* &= -\hat{I}_L \cdot \hat{\alpha}^L - \hat{\omega}^L \times (\hat{I}_L \cdot \hat{\omega}^L), \\
\hat{T}_R^* &= -\hat{I}_R \cdot \hat{\alpha}^L - \hat{\omega}^R \times (\hat{I}_R \cdot \hat{\omega}^R), \\
\hat{T}_B^* &= -\hat{I}_B \cdot \hat{\alpha}^B - \hat{\omega}^B \times (\hat{I}_B \cdot \hat{\omega}^B).
\end{aligned} \tag{40b}$$

Now, the generalized inertia forces and torques are determined by taking the inner product between the partial velocities and partial angular velocities (35) and the inertia forces and torques (40) as

$$F_r^* = \sum_{P=L,R,B} \hat{v}_r^P \cdot \hat{R}_P^* + \sum_{P=L,R,B} \hat{\omega}_r^P \cdot \hat{T}_P^* \ (r = 1 \sim 3). \tag{41}$$

As a consequence, we have

$$\begin{aligned}
F_1^* &= m_B l(\dot{\theta}^2 + \dot{\psi}^2)\,\mathrm{s}\,\theta - m_B l\ddot{\theta}\,\mathrm{c}\,\theta \\
&\quad - (m_B + 2m_W + 2J/r^2)\ddot{x}, \\
F_2^* &= -(I_3 - I_1 - m_B l^2)\dot{\psi}^2\,\mathrm{s}\,\theta\,\mathrm{c}\,\theta
\end{aligned}$$

$$
\begin{aligned}
&-m_B l\ddot{x}\,\mathrm{c}\,\theta-(I_2+m_B l^2)\ddot{\theta},\\
F_3^* &= \{2(I_3-I_1-m_B l^2)\dot{\theta}\,\mathrm{c}\,\theta-m_B l\dot{x}\}\dot{\psi}\,\mathrm{s}\,\theta\\
&\quad-\{I_3+2K+(m_W+J/r^2)d^2/2\\
&\quad-(I_3-I_1-m_B l^2)\mathrm{s}^2\,\theta\}\ddot{\psi}.
\end{aligned}
\tag{42}
$$

Finally, in Kane's mechanics, the sum of the generalized active forces and the generalized inertia forces becomes zero. Hence,

$$F_i+F_i^*=0 \quad (i=1\sim 3), \tag{43}$$

from which three equations of motion are obtained. In the sequel, they are the same as (25)-(27) derived in the Lagrangian approach.

4.3. Kane's method errors in other works

When differentiating the linear velocities in (8) and angular velocities in (9) to find the inertia forces and torques in (40), the unit vectors also must be differentiated with respect to time, and the results depend on the angular velocities of the rotating frames $\{B\}$ and $\{C\}$.

However, in [3,7,24], the unit vector differentiation process for the pendulum angular velocity was neglected because the pitch rate was wrongly described with respect to the fixed frame as $\hat{\omega}^B=\dot{\theta}\hat{n}_2+\dot{\psi}\hat{n}_3$. As a consequence, it led to modeling errors in the centrifugal and Coriolis forces. Effectively, it is the same as the c_{31} and c_{33} elements and the MOI terms in the c_{23} and c_{32} elements are removed in the centrifugal and Coriolis matrix in (29).

5. DYNAMIC CHARACTERISTICS OF 2WBMR

5.1. Effect of the mass moment of inertia

By taking the inverse of the inertia matrix in the derived equation of motion in (28), the accelerations of straight, pitch, and yaw motion can be written in the following form:

$$\ddot{x}=\frac{\mathrm{s}\,\theta}{V_1}\left(-C_{11}g+C_{12}\dot{\theta}^2+C_{13}\dot{\psi}^2\right)+C_{14}\left(T_L+T_R\right), \tag{44a}$$

$$\ddot{\theta}=\frac{\mathrm{s}\,\theta}{V_1}\left(C_{21}g-C_{22}\dot{\theta}^2-C_{23}\dot{\psi}^2\right)-C_{24}\left(T_L+T_R\right), \tag{44b}$$

$$\ddot{\psi}=\frac{\mathrm{s}\,\theta}{V_2}\left(C_{31}\dot{\theta}\dot{\psi}-m_B l\dot{x}\dot{\psi}\right)-C_{32}\left(T_L-T_R\right), \tag{44c}$$

where the coefficients V_1, V_2, C_{11}, C_{12}, C_{14}, C_{21}, C_{22}, C_{24}, C_{32} are always positive, but the signs of the remaining ones are determined by the distribution of mass MOIs depending on the robot configuration.

$$
\begin{aligned}
C_{13}&=\left\{I_2+m_B l^2+(I_3-I_1-m_B l^2)\mathrm{c}^2\,\theta\right\}m_B l,\\
C_{23}&=\left\{m_B^2 l^2+(I_3-I_1-m_B l^2)(m_B+2m_W+2J/r^2)\right\}\mathrm{c}\,\theta,\\
C_{31}&=2\left(I_3-I_1-m_B l^2\right)\mathrm{c}\,\theta.
\end{aligned}
\tag{45}
$$

Hence, not considering the wheel torque input, the straight and pitch accelerations are influenced by the centrifugal forces due to pitching and yawing as well as gravity, and the yaw acceleration is governed by the two Coriolis force terms.

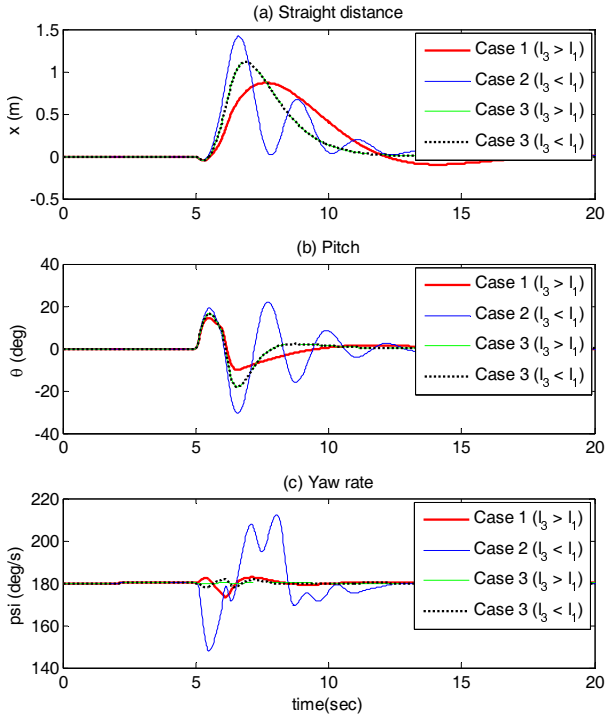

Fig. 4. Effect of the mass MOI of the inverted pendulum body.

Here, we discuss how the robot response varies according to the change of the mass moment of inertia by comparing the following three cases:

Case 1: $I_3 > I_1 + m_B l^2$, with low slenderness

Case 2: $I_3 < I_1$, with high slenderness

Case 3: I_1, I_3 neglected in (45) due to modeling error

In Case 1, we have $C_{23} > 0$, when the centrifugal force terms in the pitch acceleration (44b) always have a different sign from the gravity term. Then, the centrifugal force due to the yawing motion helps to stop the divergence of pitch angle. In Case 2, reversely, $C_{23} < 0$, when the existence of yaw rate makes the pitch angle increase more rapidly. Hence, the 2WBMRs with low slenderness are advantageous in keeping pitch stability. Actually, the same principle is applied in the rotational motion of a top. However, in Case 3 when the mass moments of inertia I_1 and I_3 are neglected in (45) due to the modeling error as in [3,7,8,24] the robot configuration will not make any difference in the dynamic response.

For the parameter values given in Table 2, we consider that the robot is spinning on a spot with the constant yaw rate of 180 deg/sec. Fig. 4 compares the responses for the three cases, where the impulsive disturbance of 10 Nm is applied to both wheels at 5 second. As a result, the Case 2 with slender body produces larger fluctuations than the Case 1 with fat body and the Case 3 shows the same responses irrespective of the MOI change.

5.2. Effect of the Coriolis terms

Except for the actuator inputs, the yaw acceleration in

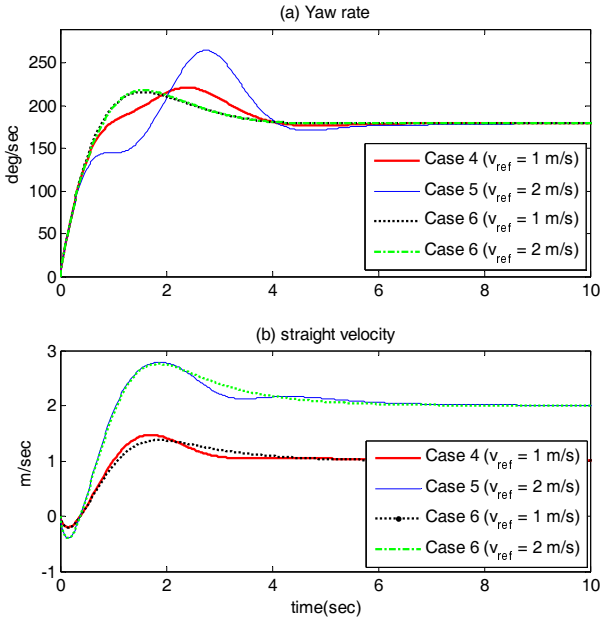

Fig. 5. Effect of the Corilois acceleration.

Table 2. 2WBMR Parameters for Simulation.

d (m)	l (m)	R (m)	m_B (kg)	m_W (kg)	J	K
0.59	0.14	0.2	41	2	0.04	0.02

(44c) is determined by the Coriolis accelerations coming from the dynamic coupling among the pitch rate, yaw rate, and forward velocity. Thus, the higher the robot speed is, the larger Coriolis effect to the yaw motion gets.

In Fig. 5, the robot arrives at the reference values of yaw rate and forward velocity for turning motion, where Case 4 and Case 5 indicate when the velocity reference is 1 m/sec and 2 m/sec, respectively, and Case 6 when the Coriolis acceleration $\dot{x}\dot{\psi}$ is neglected due to the modeling error in [3,7,22,24]. As expected, the initial responses of the yaw rate show a big difference between Case 4 and Case 5, but in Case 6, the change of velocity reference does not produce any difference in the yaw rate response.

6. CONCLUSION

As high maneuver capability of the two-wheeled balancing robot is demanded for personal transportation, industrial application, police patrol, and military use, a reliable dynamic model for performance evaluation and control design will get important as much. Currently, many articles include wrong results in their dynamic models. Although some of them are exact, only final results were given. In this regard, this paper suggests a sound understanding about how to establish the dynamic model by comparing the Lagrangian approach and Kane's method and discussing the modeling errors in the former works.

APPENDIX A

A.1. Elements of the Matrices in (29)

Note: $\mathrm{s}\theta \triangleq \sin\theta$, $\mathrm{c}\theta \triangleq \cos\theta$, $\mathrm{s}^2\theta \triangleq \sin^2\theta$, $\mathrm{c}^2\theta \triangleq \cos^2\theta$

$$a_{11} = m_B + 2m_W + 2J/r^2$$
$$a_{12} = a_{21} = m_B l\,\mathrm{c}\theta$$
$$a_{22} = I_2 + m_B l^2$$
$$a_{33} = I_3 + 2K + (m_W + J/r^2)d^2/2 - (I_3 - I_1 - m_B l^2)\mathrm{s}^2\theta$$
$$c_{12} = -m_B l\dot{\theta}\,\mathrm{s}\theta$$
$$c_{13} = -m_B l\dot{\psi}\,\mathrm{s}\theta$$
$$c_{23} = (I_3 - I_1 - m_B l^2)\dot{\psi}\,\mathrm{s}\theta\,\mathrm{c}\theta$$
$$c_{31} = m_B l\dot{\psi}\,\mathrm{s}\theta$$
$$c_{32} = -(I_3 - I_1 - m_B l^2)\dot{\psi}\,\mathrm{s}\theta\,\mathrm{c}\theta$$
$$c_{33} = -(I_3 - I_1 - m_B l^2)\dot{\theta}\,\mathrm{s}\theta\,\mathrm{c}\theta$$
$$d_{11} = 2c_\alpha / r^2$$
$$d_{12} = d_{21} = -2c_\alpha / r$$
$$d_{22} = 2c_\alpha$$
$$d_{33} = (d^2/2r^2)c_\alpha$$

REFERENCES

[1] Y. Ha and S. Yuta, "Trajectory tracking control for navigation of the inverse pendulum type self-contained mobile robot," *Robotics and Autonomous Systems*, vol. 17, pp. 65-80, 1996.

[2] F. Grasser, A. D'Arrigo, S. Colombi, and A. C. Rufer, "Joe: a mobile, inverted pendulum," *IEEE Trans. on Industrial Electronics*, vol. 49, no. 1, pp. 107-114, February 2002.

[3] Y. Kim, S. Kim, and Y. Kwak, "Dynamic analysis of a nonholonomic two-wheeled inverted pendulum robot," *Journal of Intelligent and Robotic Systems*, vol. 44, no. 1, pp. 25-46, 2005.

[4] T. Takei, R. Imamura, and S. Yuta, "Baggage transportation and navigation by a wheeled inverted pendulum mobile robot," *IEEE Trans. on Industrial Electronics*, vol. 56, no. 10, pp. 3985-3994, 2009.

[5] S. C. Lin, P. S. Tsai, and H. C. Huang, "Adaptive robust self-balancing and steering of a two-wheeled human transportation vehicle," *Journal of Intelligent and Robotic Systems*, vol. 62, no. 1, pp. 103-123, April 2011.

[6] P. Petrov and M. Parent, "Dynamic modeling and adaptive motion control of a two-wheeled self-balancing vehicle for personal transport," *Proc. of 13th Int. IEEE Conf. on Intelligent Transportation Systems*, pp. 1013-1018, 2010.

[7] H. Azizan, M. Jafarinasab, S. Behbahani, and M. Danesh, "Fuzzy control based on LMI approach and fuzzy interpretation of the rider input for two wheeled balancing human transporter," *Proc. of 8th IEEE Int. Conf. on Control and Automation*, pp. 192-197, 2010.

[8] M. Baloh and M. Parent, "Modeling and model verification of an intelligent self-balancing two-wheeled vehicle for an autonomous urban transportation system," *Proc. of the Conf. on Computational Intelligence, Robotics, and Autonomous Systems*, pp. 1-7, 2003.

[9] General Motors, [Online video]. Available: http://en.wikipedia.org/wiki/General_Motors_EN-V, http://youtu.be/zoKxx0GEEFE
[10] H. Ustal and J. L. Minkel, "Study of the independence IBOT 3000 mobility system: an innovative power mobility device, during use in community environments," *Archives of Physical Medicine and Rehabilitation*, vol. 85, no. 12, pp. 2002-2010, December 2004.
[11] Genny Mobility, [Online video]. Available: http://www.gennymobility.com/Genny/Concept.aspx, http://youtu.be/7DfcjRcoef0
[12] S. Miao and Q. Cao, "Modeling of self-tilt-up motion for a two-wheeled inverted pendulum," *Industrial Robot: An International Journal*, vol. 38, no. 1, pp. 76-85, January 2011.
[13] S. Jeong and T. Takayuki, "Wheeled inverted pendulum type assistant robot: design concept and mobile control," *Intelligent Service Robotics*, pp. 313-320, 2008.
[14] Z. Li and J. Luo, "Adaptive robust dynamic balance and motion controls of mobile wheeled inverted pendulums," *IEEE Trans. on Control Systems Technology*, vol. 17, no. 1, pp. 233-241, January 2009.
[15] C. H. Huang, W. J. Wang, and C. H. Chiu, "Design and implementation of fuzzy control on a two-wheel inverted pendulum," *IEEE Trans. on Industrial Electronics*, vol. 58, no. 7, pp. 2988-3001, July 2011.
[16] J. Huang, Z.-H. Guan, T. Matsuno, T. Fukuda, and K. Sekiyama, "Sliding mode velocity control of mobile-wheeled inverted-pendulum systems," *IEEE Trans. on Robotics*, vol. 26, no. 4, pp. 750-758, August 2010.
[17] A. Salerno and J. Angeles, "A new family of two wheeled mobile robot: modeling and controllability," *IEEE Trans. on Robotics*, vol. 23, no. 1, pp. 169-173, February 2007.
[18] K. Pathak and S. Agrawal, "Band-limited trajectory planning and tracking for certain dynamically stabilized mobile systems," *Journal of Dynamic Systems, Measurement, and Control*, vol. 128, no. 1, pp. 104-111, 2006.
[19] K. Teeyapan, J. Wang, T. Kunz, and M. Stilman. "Robot limbo: optimized planning and control for dynamically stable robots under vertical obstacles," *IEEE Int. Conf. on Robotics and Automation*, pp. 4519-4524, 2010.
[20] D. Choi and J. Oh, "Human-friendly motion control of a wheeled inverted pendulum by reduced-order disturbance observer," *Proc. of IEEE Int. Conf. on Robotics and Automation*, pp. 2521-2526, May 2008.
[21] K. Pathak, J. Franch, and S. Agrawal, "Velocity and position control of a wheeled inverted pendulum by partial feedback linearization," *IEEE Trans. on Robotic*s, vol. 21, no. 3, pp. 505-513, June 2005.
[22] M. C. Tsai and J. S. Hu, "Pilot control of an auto-balancing two wheeled cart," *Advanced Robotics*, vol. 21, no. 7, pp. 817-827, 2007.
[23] T. R. Kane and D. A. Levinson, *Dynamics: Theory and Applications*, McGraw-Hill Book Company, 1985.
[24] M. Muhammad, S. Buyamin, M. N. Ahmad, S. W. Nawawi, and A. A. Bature, "Multiple operating points model-based control of a two-wheeled inverted pendulum mobile robot," *Int. Journal of Mechanical & Mechatronics Engineering IJMME-IJENS*, vol. 13, no. 5, pp. 1-9, 2013.
[25] B. Siciliano, L. Sciavicco, L. Villani, and G. Oriolo, *Robotics: Modeling, Planning and Control*, Springer-Verlag London, 2009.

Sangtae Kim received his B.S. and M.S. degrees in Aerospace and Mechanical Engineering from Korea Aerospace University, in 2008 and 2010, respectively. He is currently working toward a Ph.D. degree in School of Aerospace and Mechanical Engineering, Korea Aerospace University. His research interests include design, analysis, and nonlinear optimal control of two-wheeled balancing mobile robot.

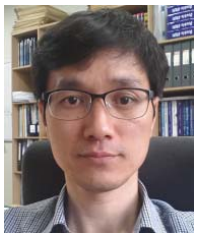

SangJoo Kwon received his B.S. degree in Naval Architecture and Ocean Engineering from Seoul National University in 1989, and his M.S. and Ph.D. degrees in Mechanical Engineering from Pohang University of Science and Technology (POSTECH), in 1991 and 2002, respectively. He was with the Agency for Defense Development of Korea from 1991 to 1997 as a Research Scientist and the Korea Institute of Science and Technology in 2003 and the Korea Institute of Industrial Technology in 2004 as a Senior Researcher. Currently, he is an Associate Professor in School of Aerospace and Mechanical Engineering, Korea Aerospace University. His current research interests include mobile robot design and control, optimal planning, and filtering.